Langmuir

Article

pubs.acs.org/Langmuir

Partitioning Behavior of Silica-Coated Nanoparticles in Aqueous Micellar Two-Phase Systems: Evidence for an Adsorption-Driven Mechanism from QCM-D and ATR-FTIR Measurements

Ingo Fischer, Christian Morhardt, Stefan Heissler, and Matthias Franzreb*

Karlsruhe Institute of Technology, Herrmann-von-Helmholtz Platz 1, 76344 Eggenstein-Leopoldshafen, Germany

Supporting Information

ABSTRACT: Quartz crystal microbalance with dissipation (QCM-D), attenuated total reflectance Fourier transform infrared spectroscopy (ATR-FTIR), and total organic carbon detection (TOC) are employed to examine the cause of the differences in the partitioning of silica-coated nanoparticles in an aqueous micellar two-phase system based on nonionic surfactant Eumulgin ES. The particles partition into the micelle-rich phase at pH 3 and into the micelle-poor phase at pH 7. Our results clearly show that the nonionic surfactants are adsorbed to the silica surface at pH 3. Above the critical temperature, a stable surfactant bilayer forms on the silica surface. At pH 7, the surfactants do not adsorb to the particle surface; a surfactant-loaded particle is therefore drawn to the micelle-rich phase but otherwise repelled from it. These results suggest that the partitioning in aqueous micellar two-phase systems is mainly driven by hydrogen bonds formed between the surfactants and the component to be partitioned.

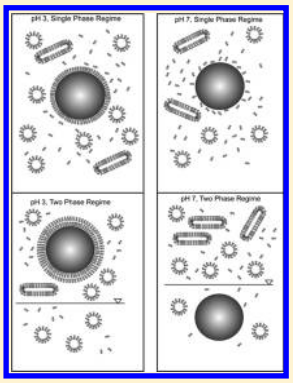

INTRODUCTION

Aqueous two-phase systems (ATPS) and aqueous micellar two-phase systems (AMTPS) can be used to concentrate proteins and other (in)soluble substances on the basis of their partitioning behavior between the two phases.[1] The mechanism of the partitioning depends on both system conditions and target molecule characteristics and is still unclear.

Much attention has been paid to the partitioning of soluble molecules in AMTPS, and it has been shown that the partitioning coefficient of a protein can be reasonably predicted by the excluded-volume theory that is mainly based on the hydrodynamic radius of the particular protein and the (growth of the) cross-sectional radius of the phase-forming micelles.[2]

The mechanism of the partitioning of colloids and insoluble particles in aqueous two-phase systems, however, has scarcely been investigated although several publications describe the macroscopic behavior of particles in two-phase systems: PEG/dextran ATPS has been used to partition Au and Ag nanospheres with sizes of less than 100 nm.[3] Here, Au nanospheres partitioned preferentially into the PEG-rich phase whereas Ag nanospheres were mainly partitioned into the dextran phase. The two-phase behavior of polymeric acrylic latex and colloidal TiO_2 particles was found to be dependent on both the surface chemistry and the size of the particles.[4] The authors emphasized the influence of the pH on the partitioning; at low pH, when the carboxylated particles were protonated, they partitioned into the PEG phase. Additionally, it was shown that the addition of silica and polystyrene latex particles to stable PEG/dextran systems induces phase separation by shifting the coexistence curve of the ATPS.[5] The authors explain their results by two different mechanisms, both originating from the adsorption from one polymer to the particles. The addition of magnetic particles as carriers for biomolecules as a tool in biopurification has been shown for ATPS[6,7] as well as for AMTPS.[8,9] Recently, the potential of AMTPS to concentrate silver, gold, and palladium nanoparticles was shown.[10−12] The authors used nonionic surfactants Triton X-114 and Triton X-100 to concentrate the nanoparticles in the micelle-rich phase of the two-phase systems. Despite the practical applicability of these studies, no mechanism of the partitioning of the nanoparticles is explained.

The purpose of our study was to investigate the mechanism of the partitioning of nanoparticles in AMTPS. As described, several authors hypothesize that the partitioning of particles in ATPS is somehow related to the adsorption of the phase-forming polymer to the particle surface. Our intention was to investigate if the partitioning of particles in AMTPS is based on the same principle and if so to investigate the mechanism of adsorption.

Silica-coated Fe_3O_4 nanoparticles with a mean size of 100 nm were tested. The partitioning of the particles in AMTPS based on nonionic surfactant Eumulgin ES was investigated at different pH levels as well as in the presence and absence of chaotropic organic molecule urea; the correlation of the partitioning behavior of the particles and the adsorption of surfactant to the silica surface was monitored by quartz crystal microbalance with dissipation (QCM-D). Reference chips with silica surfaces were used under the same conditions as those in

Received: August 15, 2012
Revised: October 16, 2012
Published: October 18, 2012

the partitioning experiments. In addition, the adsorptive behavior of the phase-forming surfactant onto the particles was directly detected by attenuated total reflectance Fourier transform infrared spectroscopy (ATR-FTIR) and by surfactant-binding studies.

EXPERIMENTAL SECTION

Materials. *Chemicals.* All chemicals were analytical grade and used without further purification. All water used was prepared with a Milli-Q system (Millipore, USA). Ethanol and citric acid monohydrate were purchased from Merck Millipore (Darmstadt, Germany); disodium phosphate, sodium dodecyl sulfate, hydrochloric acid, and sodium hydroxide were purchased from Carl Roth (Karlsruhe, Germany); and sodium lactate was purchased from AppliChem (Darmstadt, Germany). Nonionic surfactant Eumulgin ES (PPG-5-laureth-5, CAS no. 68439-51-0) was purchased from Cognis (Düsseldorf, Germany). The density of Eumulgin ES was determined with a DCAT 11 system (Dataphysics, Filderstadt, Germany) and resulted in ρ = 982 kg/m^3. The average length of an Eumulgin ES molecule, C12-(POE)5-(POP)5, was calculated to be 5.57 nm using Yasara software, version 12.4.1.[13] The hydrodynamic diameter of a 0.5% Eumulgin ES solution in both 20 mM sodium phosphate at pH 7 and 20 mM sodium citrate at pH 3 was determined by dynamic light scattering (DLS) by means of a Zetasizer 5000 (Malvern Instruments GmbH, Herrenberg, Germany) to be 15 nm.

Particles. MagPrep silica particles were obtained from Merck Millipore (Darmstadt, Germany). The particles consist of magnetite (Fe_3O_4) monocrystals with a thin silica coating. Scanning electron microscope (SEM) pictures reveal a mean diameter of single particles of 100 nm with a narrow size distribution.

Methodology. *Partitioning Experiments.* Initially, an Eumulgin ES-based AMTPS phase diagram was prepared in 20 mM sodium citrate at pH 3 following a protocol described elsewhere.[14] The Eumulgin ES solution was heated to a temperature above the cloud point, and the temperature was maintained until the phases were separated. The surfactant concentrations of both emerging phases were determined by potentiometric titration and subsequently plotted on a T, x diagram.

The partitioning of the MagPrep silica particles in Eumuling ES-based AMTPS was investigated with regard to the pH of the AMTPS solution. Therefore, Eumulgin ES AMTPS was set up in 20 mM solutions of sodium citrate, sodium phosphate, and sodium lactate. The pH was titrated to the respective value with hydrochloric acid or sodium hydroxide. To investigate the influence of urea, additional AMTPS consisting of 20 mM sodium citrate and 6 M urea was created. In all experiments, the Eumulgin ES concentration was 10 wt %.

Initially, the particles were equilibrated in the corresponding buffer and then added to the AMTPS. The final particle concentration in the AMTPS was set to 0.5 g/L. After temperature-induced phase separation, the particle partitioning behavior was observed visually. The phase-separation temperature was set to 30 °C in all experiments except for the experiments that were carried out with urea; in these experiments, the temperature had to be elevated to 35 °C to induce phase separation.

Quartz Crystal Microbalance. The QCM-D experiments were performed using a Q-Sense E4 system with Qsoft 401 software (Q-Sense, Gothenburg, Sweden). QCM-D exploits the piezoelectric effect in chips composed of an AT-cut, disk-shaped, polished quartz crystal, which has a fundamental frequency of 4.95 MHz. QCM-D monitors the adsorption of molecules onto the surface of the chip because of a negative shift in frequency (f) that is proportional to the mass on the crystal. In addition, there is a positive shift in dissipation (D) proportional to the viscoelastic properties of that mass. QCM-D measurements relate the mass to the frequency shift based on the work of Sauerbrey[15] according to eq 1

$$\Delta m = -\frac{C\Delta f}{n} \tag{1}$$

where m is the adsorbed mass, Δf is the frequency shift, n = 1, 3, 5...13 being the observed overtone, and C = 17.7 ng Hz^{-1} cm^{-2} being the mass sensitivity constant of the crystal. The average thickness of the adsorbed surfactant layer was calculated using eq 2

$$t_{\text{eff}} = \frac{\Delta m}{\rho_{\text{eff}}} \tag{2}$$

where ρ_{eff} is the densitiy of Eumulgin ES and t_{eff} is the thickness of the adsorbed film.

Silica-coated chips (QSX 303, Q-Sense, Gothenburg, Sweden) were used for the QCM-D measurements. To clean the chips, they were sonicated in ethanol for 10 min, dried with nitrogen, and irradiated with UV ozone (ProCleaner, Bioforce Nanoscience, Ames, IA) for 10 min. After the experiments, the chips were sonicated in ethanol for 10 min and two times in Milli-Q water, dried with nitrogen, and stored under ambient conditions. All chips were used multiple times.

During all experiments, the flow rate was set to 50 μL/min. All experimental conditions were designed to meet the same conditions as in the partitioning experiments: temperatures were set to either 20 °C to simulate a single-phase temperature or to 30 °C (to 35 °C in the case of the urea experiments) to generate phase-separation conditions. The buffers used were the same as described in the partitioning experiments. Initially, the chips were equilibrated in the corresponding buffer; after a stable baseline was achieved, the buffered 10 wt % surfactant solution was injected. Rinsing with the surfactant solution was performed for at least 45 min, and afterwards a pure buffer was injected until a constant signal was reached. Finally, the system was rinsed with Milli-Q water.

Surfactant Binding and Elution Studies. Merck MagPrep silica solutions were prepared as follows: 10 mL samples containing a particle concentration of 10 g/L were prepared; these samples contained 10 wt % Eumulgin ES at either pH 3 or 7. All solutions were buffered using sodium phosphate. Each sample was kept constant at 4 °C or at 30 °C. This setup resulted in a total of four different samples: pH 3 or 7 at 4 or 30 °C. All experiments were performed in triplicate. The samples were initially incubated in an overhead shaker for 20 min in 10% Eumulgin ES at the respective pH and temperature. Afterwards, the particles were separated from the Eumulgin ES solution using a hand magnet. Then particles were washed in 10 mL of pure buffer at the respective temperature and pH for 20 min. The supernatant was again separated from the particles. The washing procedure was repeated for an additional 11 times, resulting in a total 12 washings. All samples were analyzed for their Eumulgin ES content by a determination of the total organic carbon.

Surfactant Determination by TOC. The surfactant concentration in the samples was determined by the detection of the total organic carbon using the Multi N/C 2000 (Analytik Jena, Jena, Germany). Fifteen microliters of hydrochloric acid was added to each sample before TOC measurements in order to remove dissolved inorganic carbon. The total surfactant concentration was calculated from the TOC content; the carbon mass makes up for 63.8% of the total mass of nonionic surfactant Eumulgin ES.

Surfactant–Particle Investigation with ATR-FTIR. For the ATR-FTIR measurements, a Tensor 27 IR spectrometer with a Platinum ATR (single reflecting diamond) accessory (Bruker Optics, Ettlingen, Germany) was used. Each spectrum comprised 64 coadded scans with a spectral resolution of 4 cm^{-1} in the 3600–400 cm^{-1} range. The data was acquired using OPUS 6.5 software (Bruker Optics, Ettlingen, Germany).

The MagPrep silica particles were equilibrated in a citrate buffer at pH 3 or phosphate buffer at pH 7 and then incubated in the same buffer containing 10% Eumulgin ES. Afterwards, the particles were washed five times in the pure buffer.

The particle suspensions were applied to the ATR crystal and allowed to dry for 10 min. The spectra of the plain particles were subtracted from spectra of the processed particles. The spectra were baseline corrected by a concave rubber band method.

dx.doi.org/10.1021/la303313m | Langmuir 2012, 28, 15789–15796

RESULTS AND DISCUSSION

Phase Diagram of Eumulgin ES-Based AMTPS. The unique properties of AMTPS in a certain buffer are characterized by its phase diagram. Figure 1 depicts the phase

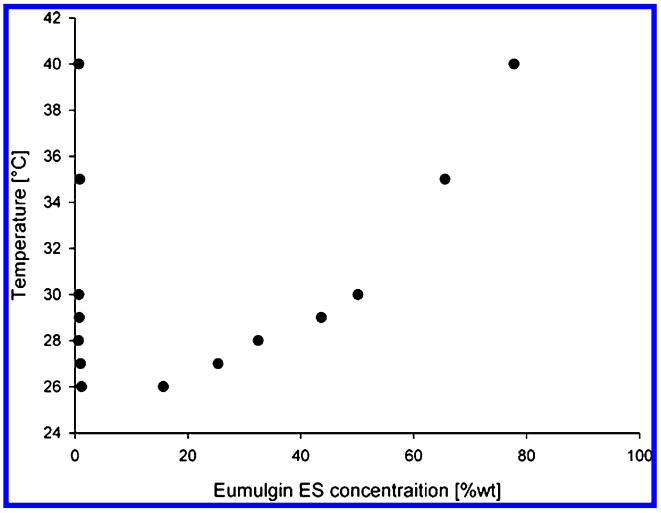

Figure 1. Phase diagram of a 20 mM sodium citrate Eumulgin ES AMTPS. The points of transition from a single-phase to a two-phase state are shown. The phase separation depends on the surfactant concentration and the temperature.

diagram of AMTPS of Eumulgin ES in 20 mm sodium citrate. Phase diagrams of Eumulgin ES AMTPS have been determined in water and 100 mM sodium phosphate at pH 7.[14] From the comparison of the phase diagrams, it can be seen that the pH and salt concentrations within the investigated range have little influence on the phase diagram and thus on the intermicellar interactions. It is generally assumed that the phase separation of AMTPS is based on the temperature-induced growth of the nonionic micelles. With increasing temperature, the micelles grow until a thermodynamically favored phase separation occurs. This phenomenon has been fundamentally investigated by a work group around Blankschtein.[16,17]

The dots represent the temperature where the system starts to split into two phases.

Partitioning Experiments. The partitioning of silica-coated 100 nm Fe_3O_4 particles in an Eumulgin ES-based AMTPS was investigated. At pH 3 and 4, the particles partition into the micelle-rich phase, independent of the buffer used. At pH 7, the particles partition completely into the micelle-poor phase. In all cases, the volume fraction of the micelle-rich top phase was 20% of the total volume at 35 °C.

Figure 2 illustrates the difference between magnetic particles in the single-phase regime at a low temperature and after phase separation, accumulating in the micelle-rich top phase and micelle-poor bottom phase, respectively.

By changing the buffer composition and/or the pH, we change the ionic strength of the solution. The effect of the ionic strength in AMTPS systems, however, results in an increasing or decreasing shift of the phase diagram, depending on the kind and especially the concentration of the applied salt. For chaotrophic agents, the phase-separation temperature (the cloud point) is decreased, but for cosmotrophic agents, the cloud point is increased.[18] To exclude the contribution of the particular salt from the partitioning behavior (e.g., at pH 3), the partitioning experiments were carried out in the presence of

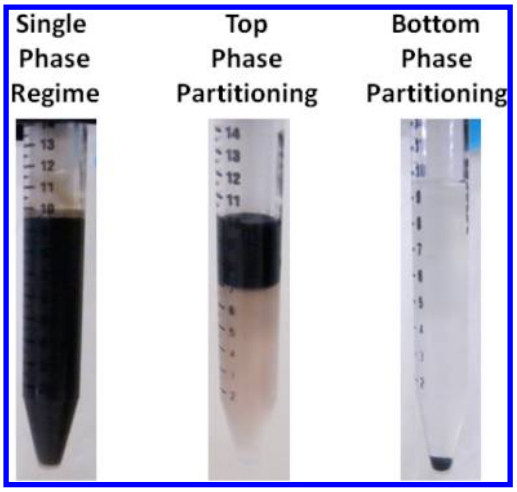

Figure 2. Possibilities of the partitioning behavior of 100 nm silica particles in an Eumulgin ES-based AMTPS: (left) in a single-phase state, the particles are homogenously distributed in the solution; (middle) the particles partition into the micellar-rich top phase; and (right) the particles partition into the micelle-poor bottom phase and sediment on the bottom.

two different buffering salts, viz., sodium phosphate and sodium citrate. In both cases, the partitioning of the particles did not diverge. Phase diagrams of Eumulgin ES have been investigated in 100 mM sodium phosphate and in pure water.[14] From these diagrams, it can be seen that the influence of pH in the investigated range on the phase diagram and thus on the aggregation behavior of the surfactants at the investigated salt concentrations even at different pH values is small. Therefore, the correlation among the nonionic surfactant, particle surface, and pH must be responsible for the partitioning behavior. The interactions of polyoxyethylated nonionic surfactants or poly(oxyethylene oxide) and hydrophilic surfaces, however, have been described extensively.[19−21] It is generally accepted that the interactions are mainly driven by hydrogen bonds that form between the ether oxygens or the hydroxyl end of the nonionic surfactant and the hydrophilic surface.[22] Therefore, a lower pH increases the protonation of the OH groups of either the surface or surfactant, leading to the adsorption of the nonionic surfactants to the surface.[23,24] For this reason, particles in the micellar-rich top phase are stabilized by the adsorption of the surfactant onto their surface, which prevents particle aggregation, and the particles agglomerate and sediment to the bottom phase when the surfactants do not adsorb.

To investigate the role of hydrogen bonds in the mechanism of the partitioning behavior of the silica-coated sorbents, AMTPS containing high concentrations of urea has been set up. Urea is known to have a strong impact on the solvent−solute interaction and the micellar properties of AMTPS (e.g., increasing the critical micelle concentration[25] and the cloud point[18,26]). In general, the role of urea is related to its direct interaction with the hydrogen bonds between water molecules or by the interaction of urea with the solute. Recent experimental findings support the latter theory, which now has become widely accepted.[27,28]

The addition of urea reverses the partitioning behavior of the 100 nm Fe_3O_4 silica particles from the micelle-rich to the micelle-poor phase in a 20 mM sodium citrate system at pH 3. This effect can be explained by the inference of urea with the

dx.doi.org/10.1021/la303313m | Langmuir 2012, 28, 15789−15796

hydrogen bonds of the nonionic surfactant and the silica surface. When the nonionic surfactants do not adsorb onto the particles, they are excluded from the micellar-rich phase of the system.

Surfactant Binding on Reference Surfaces. Quartz crystal microbalance signals were recorded in order to monitor the surfactant−SiO_2 interaction at different pH values at different temperatures.

Initially, each silica chip was equilibrated in the respective buffer and then rinsed with the Eumulgin ES solution. Figure 3 shows an example of the real-time signal curve for overtones five, seven, and nine at 20 °C and pH 3.

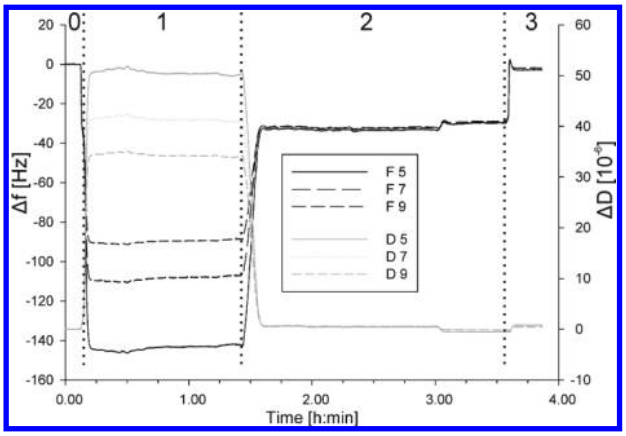

Figure 3. QCM-D signal obtained during the rinsing of a silica chip with sodium citrate and Eumulgin ES at pH 3 and 20 °C. The silica chip is rinsed with (0) sodium citrate, (1) 10% Eumulgin ES in sodium citrate, (2) sodium citrate, and (3) Milli-Q water. The signal shift to −35 Hz is generated by a Eumulgin ES monolayer that is adsorbed to the silica surface. When the chip is rinsed with Milli-Q water, the Eumulgin ES layer is removed completely.

The signals for Δf decrease and those for ΔD increase when the chip is in contact with the surfactant solution, yet the frequency shifts do not run congruently. This is due to the fact that the solution rinsing the chip behaves like a viscoelastic film because of the high surfactant concentration. An increased shift in energy dissipation also arises from this effect. When the SiO_2 surface is rinsed with buffer containing no surfactant, a stable frequency shift of approximately −35 Hz occurs for all overtones. The dissipation is decreased close to zero. In this state, a stable rigid surfactant layer is adsorbed to the SiO_2 surface. When the surface is rinsed with Milli-Q water, the surfactant layer is desorbed and the signal drops back to zero.

Figure 4 displays the QCM-D signal for the experiment at pH 7 at 20 °C.

When the silica chip is rinsed with the surfactant solution, the signal change is similar to the signal change at pH 3, yet when the SiO_2 surface is rinsed with pure buffer, the frequency signal drops to zero immediately. Rinsing the silica chip with Milli-Q water does not change the signal. In conclusion, at pH 7 no surfactant layer is adsorbed to the SiO_2 surface. The signal change by rinsing with surfactant solution is due to the interaction or loose attachment of the surfactant to the silica surface.

When the temperature is increased to 30 °C, the cloud point of the Eumulgin ES solution is crossed and the system splits. QCM-D signals for a solution heated to 30 °C at pH 3 are shown in Figure 5.

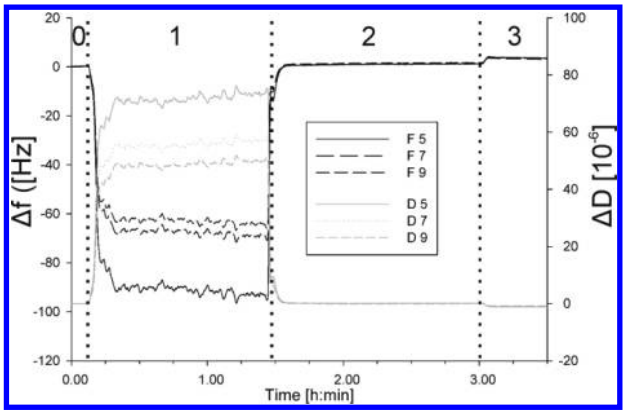

Figure 4. QCM-D signal obtained during the rinsing of a silica chip with sodium phosphate and Eumulgin ES at pH 7 and 20 °C. The silica chip is rinsed with (0) sodium phosphate, (1) 10% Eumulgin ES in sodium phosphate, (2) sodium phosphate, and (3) Milli-Q water. Eumulgin ES is completely removed from the chip surface after it is rinsed with sodium phosphate.

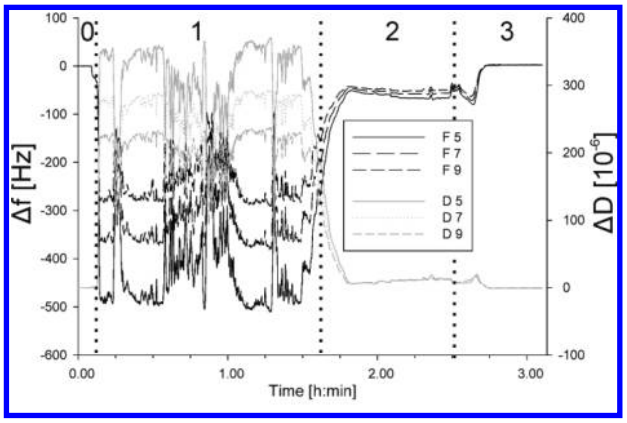

Figure 5. QCM-D signal obtained during rinsing a silica chip with sodium citrate and Eumulgin ES at pH 3 and 30 °C. The silica chip is rinsed with (0) sodium citrate, (1) 10% Eumulgin ES in sodium citrate, (2) sodium citrate, and (3) Milli-Q water. A signal shift of −55 Hz emerges when the surface is flushed with sodium citrate. The signal comes from a stable surfactant double layer formed on the silica surface at pH 3 and 30 °C.

When rinsing with the surfactant solution, fluctuations in the signal can be detected. These occur because of the inhomogeneous solution that is used to rinse the SiO_2 surface. Above the phase-separation temperature, large micelles are formed that interact with the quartz surface in an uncoordinated manner. When the surface is flushed with pure buffer, however, a constant frequency shift signal of about −55 Hz emerges. Rinsing with Milli-Q water decreases the frequency shift to zero. This effect is explained by a two-step mechanism. In the first step, the surfactants adsorb to the SiO_2 surface because of hydrogen bonding (shown in the 20 °C experiment). When the temperature is increased, the hydrocarbon chains of the surfactants congregate; the surfactants form a stable double layer on the SiO_2 surface.

In contrast to that, Figure 6 shows the signal of the QCM-D when the heated surfactant solution is brought into contact with the silica surface at pH 7. When the chip is rinsed with buffer after contact with surfactant, the signal drops to zero. Although the surfactants congregate, they do not bind to the

dx.doi.org/10.1021/la303313m | *Langmuir* 2012, 28, 15789−15796

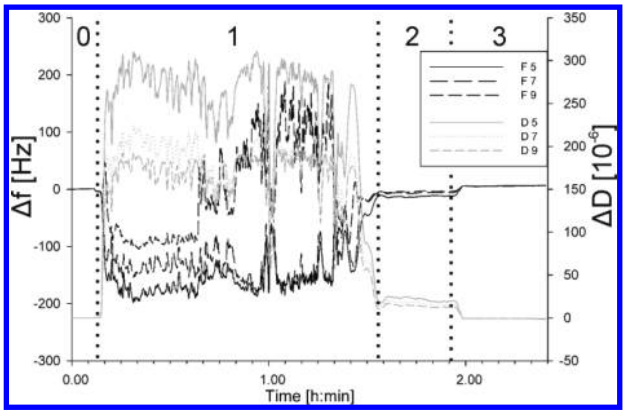

Figure 6. QCM-D signal obtained from rinsing a silica chip with sodium phosphate and Eumulgin ES at pH 7 and 30 °C. The silica chip is rinsed with (0) sodium phosphate, (1) 10% Eumulgin ES in sodium phosphate, (2) sodium phosphate, and (3) Milli-Q water. Eumulgin ES is completely removed from the chip surface after it is rinsed with sodium phosphate at 30 °C.

silica surface because no hydrogen bonding between polar heads of the surfactant and SiO_2 occurs.

When urea is added to the buffered solution at pH 3, the QCM-D signal is straight, as can be seen in Figure 7.

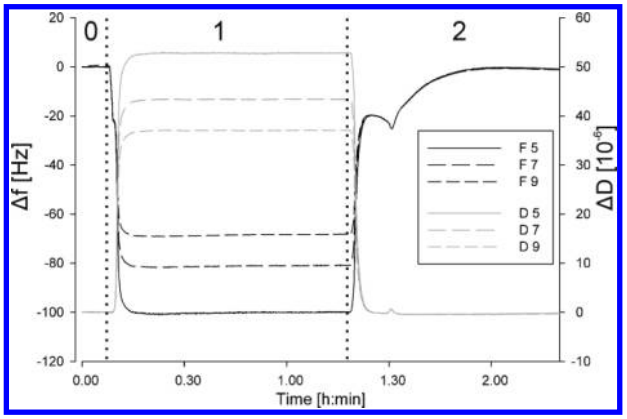

Figure 7. QCM-D signal obtained during rinsing a silica chip with sodium citrate, 6 M urea, and Eumulgin ES at pH 3 at 20 °C. The silica chip is rinsed with (0) sodium citrate, 6 M urea, pH 3; (1) 10% Eumulgin ES in sodium citrate, 6 M urea, pH 3; and (2) sodium citrate, 6 M urea, pH 3. Eumulgin ES is completely removed from the chip surface after rinsing with the buffered urea solution.

Urea stabilizes the micelles; this results in a less-staggered QCM-D signal. When rinsed with buffer and urea but without the surfactant at pH 3, the frequency shift drops to zero. When the temperature is increased to 35 °C to induce phase separation conditions and the chip is rinsed with buffer and urea after contact with the surfactant solution, the signals of both the frequency shift and dissipation slowly converge to zero. The signal curve can be seen in Figure 8. It can be concluded that Eumulgin ES does not bind permanently to the silica surface at pH 3 in the presence of 6 M urea.

The average thickness of the surfactant layers on the silica surfaces were calculated according to eqs 1 and 2. The results are summarized in Tables 1 and 2.

At 20 °C, the average thickness of the surfactant layer is 5.5 nm, and at 30 °C, the thickness was calculated to be 11.1 nm. The length of an Eumulgin ES molecule was estimated to be

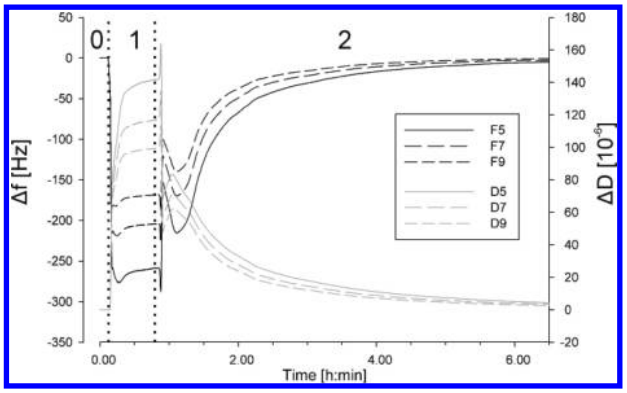

Figure 8. QCM-D signal obtained during rinsing a silica chip with sodium citrate, 6 M urea, and Eumulgin ES at pH 3 at 35 °C. The silica chip is rinsed with (0) sodium citrate, 6 M urea, pH 3; (1) 10% Eumulgin ES in sodium citrate, 6 M urea, pH 3; and (2) sodium citrate, 6 M urea, pH 3. The obtained signals converge to zero; no surfactant is adsorbed permanently to the silica surface.

Table 1. Calculated Thicknesses of the Eumulgin ES Layers on Silica Chips under Different Buffer Conditions at 20° C[a]

buffer pH/salt	thickness of adsorbed surfactant layer (nm)	standard deviation (nm)
pH 3	5.50	0.34
pH 3, 6 M urea	0.23	0.02
pH 7	0.01	0.17

[a]Calculations were made using the experimental QCM-D results and eqs 1 and 2.

Table 2. Calculated Thicknesses of the Eumulgin ES Layers on Silica Chips under Different Buffer Conditions at 30° C[a]

buffer pH/salt	thickness of adsorbed surfactant layer (nm)	standard deviation (nm)
pH 3	11.14	1.04
pH 3, 6 M urea	0.95	0.04
pH 7	0.01	1.00

[a]Calculations were made using the experimental QCM-D results and eqs 1 and 2.

5.5 nm. Therefore, it can be concluded that the surfactant molecules do not adsorb in an outstretched horizontal fashion onto the silica surface, but they are oriented vertically, with carbon chains extended toward the liquid and polar heads toward the SiO_2 surface. The addition of urea at pH 3 prevents the permanent surfactant binding completely. As discussed, at pH 7 the surfactants do not bind to the SiO_2 surface, either at 20 °C or at 30 °C.

Surfactant Binding on Particle Surfaces. MagPrep silica particles were incubated with a buffered surfactant solution at pH 3 and 7 and washed with buffer in the respective pH for 12 wash cycles. The surfactant concentrations in the wash fractions were analyzed by TOC. Figure 9 shows the concentrations in the wash fractions for wash cycles 4 to 12 performed at 4 and 30 °C.

Although at 4 °C and pH 7 the surfactant is completely eluted from the MagPrepSilica particles after five cycles, at pH 3 the attraction of the silica surface to the surfactant is stronger and up to nine wash cycles are required. This effect is even more prominent when the particles are incubated with surfactant at 30 °C as shown in Figure 9B.

dx.doi.org/10.1021/la303313m | Langmuir 2012, 28, 15789−15796

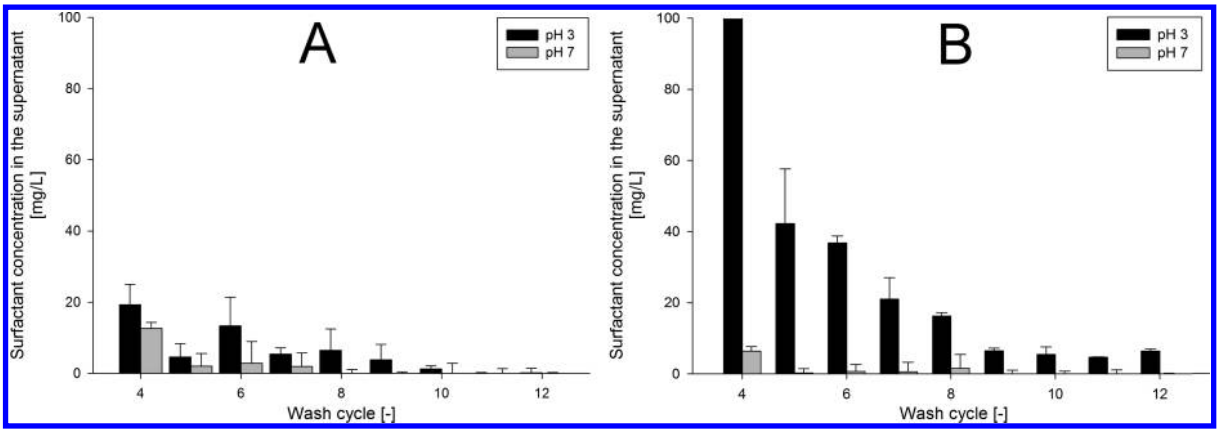

Figure 9. (A) Eumulgin ES desorbed from MagPrep silica particles in 12 wash cycles at 4 °C. Desorption was performed at 4 °C and at pH 3 or 7. Surfactant concentrations in the wash solutions are shown from cycles 4 to 12. At pH 3, the attraction of the surfactant to the SiO_2 surface is stronger. (B) Eumulgin ES desorbed from MagPrep silica particles in 12 wash cycles at 30 °C. Desorption was performed at 30 °C and at pH 3 or 7. Surfactant concentrations in the wash solutions are shown from cycles 4 to 12. At pH 3, the attraction of the surfactant to the surface is much stronger. Eumulgin ES is eluted from the particles after 12 wash cycles, and at pH 7 the surfactant is completely removed from the particles after four wash cycles.

At 30 °C and pH 7, the surfactant is removed completely after five wash cycles, and at pH 3, Eumulgin ES desorption from the particles is not completed after 12 wash cycles. In summary, at pH 3 the attraction of the nonionic surfactant to the SiO_2-coated particles is stronger at pH 3 than at pH 7. These findings are in accordance with the results obtained from the QCM-D experiments and the reference surfaces.

ATR-FTIR Spectroscopy. The sorption of Eumulgin ES onto MagPrep silica particles at pH 3 and 7 was compared by ATR-FTIR. The particles were first incubated under AMTPS conditions; afterwards, the particles were washed five times in the same buffer. ATR-FTIR spectra were taken from the plain particles, particles incubated with AMTPS, and particles that were washed five times with pure buffer after incubation. The spectra of the plain particles were subtracted from the spectra of the incubated and rinsed particles, and the results are depicted in Figures 10 and 11.

When the particles are incubated with AMTPS, the surfactants are attached to their surface; this can be observed

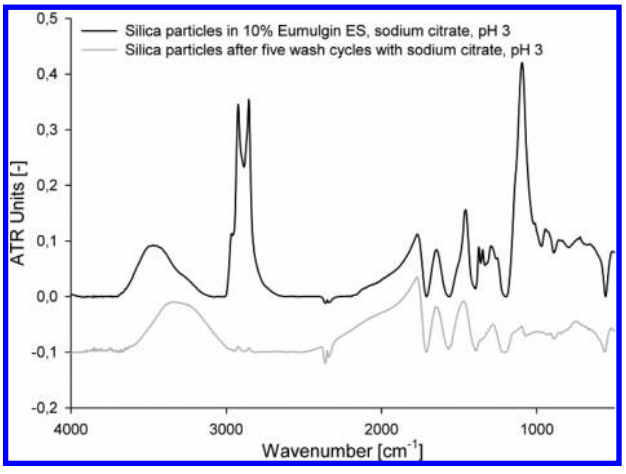

Figure 10. ATR-FTIR spectra of MagPrep silica particles incubated with Eumulgin ES at pH 3. The peaks at 2800−2950 cm^{-1} are generated from CH_2 and CH_3 stretching caused by surfactant hydrocarbon chains at the particle surface. Peaks can still be observed on the particle surface after five wash cycles at pH 3.

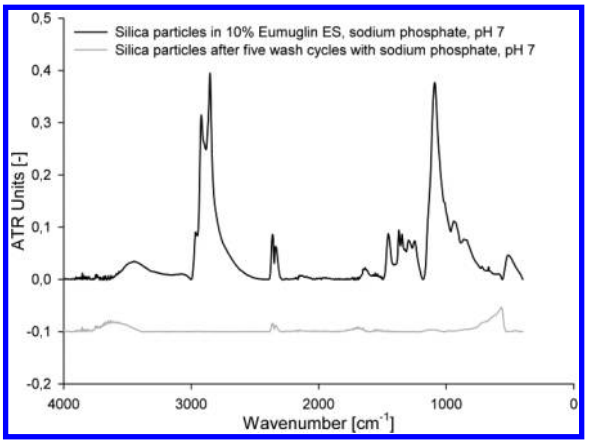

Figure 11. ATR-FTIR spectra of MagPrep silica particles incubated with Eumulgin ES at pH 7. The peaks at 2800−2950 cm^{-1} are generated from CH_2 and CH_3 stretching caused by surfactant hydrocarbon chains at the particle surface. These peaks cannot be observed on the particle surface after five wash cycles at pH 7.

by the peaks at wavenumber 2800 cm^{-1}, which are caused by stretching vibrations of their CH_2 and CH_3 groups. However, when washed at neutral pH 7, the surfactants are removed completely because no peaks can be seen in Figure 11. At pH 3, however, after five wash cycles, the peaks at 2800 cm^{-1} can still be detected. The ATR-FTIR experiments confirm the findings from the QCM-D and direct surfactant elution experiments. The surfactant is completely removed from the SiO_2 at pH 7 because the surfactants are not strongly adsorbed to the surface.

CONCLUSIONS

The correlations of the pH level, surfactant adsorption, and partitioning of silica-coated particles in an aqueous micellar two-phase system have been examined.

We have shown that at low pH the surfactants physically adsorb to the SiO_2 layer of both the particle and reference surface. Because the surfactant has a nonionic nature, these interactions seem to be hydrogen bonds formed between SiO_2 and the polar head of the surfactant. The sorption of the surfactant has been investigated using three independent methods: QMC-D based on a reference silica chip, the direct

dx.doi.org/10.1021/la303313m | Langmuir 2012, 28, 15789−15796

determination of surfactant concentration in solution, and ATR-FTIR on the particle surface. QCM-D results suggest that the nonionic surfactant adsorbs to the silica surface with its polar head toward the SiO_2 layer. When the temperature is increased, a stable double layer is formed on the silica surface.

Under the same conditions when the surfactants adsorb onto the silica surface, the particles partition into the micelle-rich phase of the system. On the contrary, under conditions when the surfactants attach only loosely to the surface, the particles partition to the micelle-poor phase of the micellar two-phase system.

We therefore propose that the partitioning of particles in micellar two-phase systems is driven by the adsorption of the phase-forming surfactant to the component to be partitioned. Figure 12 illustrates the proposed mechanism of the partitioning behavior of particulates in an aqueous micellar two-phase system.

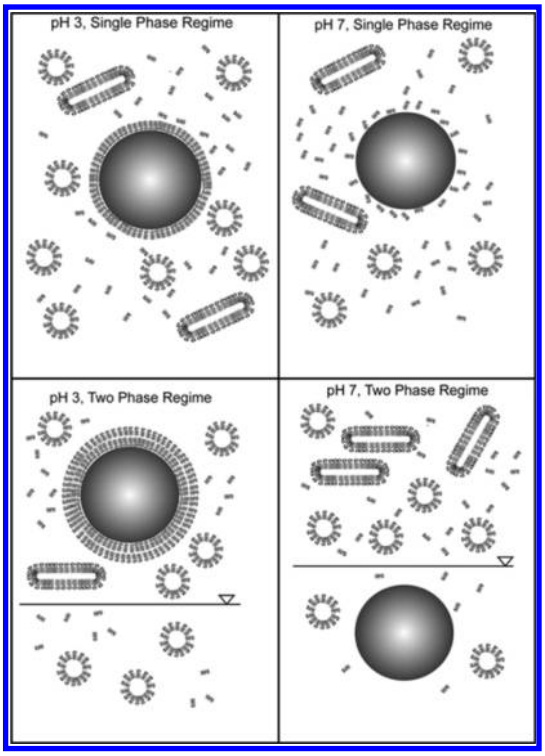

Figure 12. Mechanism of the partitioning of an insoluble particle in AMTPS. If the phase-forming surfactant adsorbs to the particle, then it is drawn to the micelle-rich phase. If the surfactant does not adsorb to the particle surface, then the particle is expelled from the micelle-rich phase.

Whenever the phase-forming surfactant covers the particle surface, these particles enter the micelle-rich phase; if the surfactant is not adsorbed to the particle surface, then the particle is excluded from the micelle-rich phase. Similar results have also been discovered for proteinaceous solutions.[29] The authors used negatively charged mixed micelles to increase the partitioning coefficient of positively charged proteins to the micelle-rich phase.

Our experimental results suggest that the partitioning of soluble and insoluble nanosized particles is based on the very same principles; hydrogen bonds formed between the phase-forming component and the component to be partitioned seem to dominate the partitioning behavior of the component in an aqueous micellar two-phase system.

■ ASSOCIATED CONTENT

Supporting Information

Phase diagram of an Eumulgin ES-based AMTPS in 100 mm sodium phosphate at pH 7. This material is available free of charge via the Internet at http://pubs.acs.org.

■ AUTHOR INFORMATION

Corresponding Author

*E-mail: matthias.franzreb@kit.edu.

Author Contributions

This article was written through the contributions of all authors. All authors have given approval to the final version of the article.

Notes

The authors declare no competing financial interest.

■ ACKNOWLEDGMENTS

We thank Dr. S. Oelmeier for the calculation of the length of the Eumulgin ES molecule and the European Commission Seventh Framework Programme "Advances Magnetic Nano-Particles Deliver Smart Processes and Products for Life - MagPro2Life" (CP-IP 229335-2) for their financial support.

■ ABBREVIATIONS

AMTPS, aqueous micellar two-phase system; ATR-FTIR, attenuated total reflectance Fourier transform infrared; QCM-D, quartz crystal microbalance with dissipation

■ REFERENCES

(1) Albertsson, P. A. *Partition of Cell Particles and Macromolecules*; John Wiley and Sons: New York, 1986.

(2) Nikas, Y. J.; Liu, C. L.; Srivastava, T.; Abbott, N. L.; Blankschtein, D. Protein Partitioning in 2-Phase Aqueous Nonionic Micellar Solutions. *Macromolecules* **1992**, *25*, 4797−4806.

(3) Helfrich, M. R.; El-Kouedi, M.; Etherton, M. R.; Keating, C. D. Partitioning and Assembly of Metal Particles and Their Bioconjugates in Aqueous Two-Phase Systems. *Langmuir* **2005**, *21*, 8478−8486.

(4) Baxter, S. M.; Sperry, P. R.; Fu, Z. W. Partitioning of Polymer and Inorganic Colloids in Two-Phase Aqueous Polymer Systems. *Langmuir* **1997**, *13*, 3948−3952.

(5) Olsson, M.; Joabsson, F.; Piculell, L. Particle-Induced Phase Separation in Mixed Polymer Solutions. *Langmuir* **2005**, *21*, 1560−1567.

(6) Suzuki, M.; Kamihira, M.; Shiraishi, T.; Takeuchi, H.; Kobayashi, T. Affinity Partitioning of Protein-a Using a Magnetic Aqueous 2-Phase System. *J. Ferment. Bioeng.* **1995**, *80*, 78−84.

(7) Gai, Q.; Qu, F.; Zhang, T.; Zhang, Y. Integration of Carboxyl Modified Magnetic Particles and Aqueous Two-Phase Extraction for Selective Separation of Proteins. *Talanta* **2011**, *85*, 304−309.

(8) Becker, J. S.; Thomas, O. R. T.; Franzreb, M. Protein Separation with Magnetic Adsorbents in Micellar Aqueous Two-Phase Systems. *Sep. Purif. Technol.* **2009**, *65*, 46−53.

(9) Fischer, I.; Franzreb, M. Nanoparticle Mediated Protein Separation in Aqueous Micellar Two-Phase Systems. *Solvent Extr. Ion Exch.* **2012**, *30*, 1−16.

(10) Liu, J. F.; Liu, R.; Yin, Y. G.; Jiang, G. B. Triton X-114 Based Cloud Point Extraction: a Thermoreversible Approach for Separation/Concentration and Dispersion of Nanomaterials in the Aqueous Phase. *Chem. Commun.* **2009**, 1514−1516.

(11) Liu, J. F.; Chao, J. B.; Liu, R.; Tan, Z. Q.; Yin, Y. G.; Wu, Y.; Jiang, G. B. Cloud Point Extraction as an Advantageous Preconcentra-

tion Approach for Analysis of Trace Silver Nanoparticles in Environmental Waters. *Anal. Chem.* **2009**, *81*, 6496−6502.
(12) Nazar, M. F.; Shah, S. S.; Eastoe, J.; Khan, A. M.; Shah, A. Separation and Recycling of Nanoparticles Using Cloud Point Extraction with Non-Ionic Surfactant Mixtures. *J. Colloid Interface Sci.* **2011**, *363*, 490−496.
(13) Krieger, E.; Koraimann, G.; Vriend, G. Increasing the Precision of Comparative Models with YASARA NOVA - A Self-Parameterizing Force Field. *Proteins: Struct., Funct., Genet.* **2002**, *47*, 393−402.
(14) Fischer, I.; Franzreb, M. Direct Determination of the Composition of Aqueous Micellar Two-Phase Systems (AMTPS) Using Potentiometric Titration-A Rapid Tool for Detergent-Based Bioseparation. *Colloids Surf., A* **2011**, *377*, 97−102.
(15) Sauerbrey, G. Verwendung Von Schwingquarzen zur Wagung Dunner Schichten und zur Mikrowagung. *Z. Phys.* **1959**, *155*, 206−222.
(16) Blankschtein, D.; Thurston, G. M.; Benedek, G. B. Theory of Phase-Separation in Micellar Solutions. *Phys. Rev. Lett.* **1985**, *54*, 955−958.
(17) Blankschtein, D.; Thurston, G. M.; Benedek, G. B. Phenomenological Theory of Equilibrium Thermodynamic Properties and Phase-Separation of Micellar Solutions. *J. Chem. Phys.* **1986**, *85*, 7268−7288.
(18) Briganti, G.; Puvvada, S.; Blankschtein, D. Effect of Urea on Micellar Properties of Aqueous-Solutions of Nonionic Surfactants. *J. Phys. Chem.* **1991**, *95*, 8989−8995.
(19) Keith, S.; Rochester, C. H. Infrared Study of the Adsorption of C12e5 on Silica Immersed in Carbon-Tetrachloride. *J. Chem. Soc., Faraday Trans. 1* **1988**, *84*, 3641−3647.
(20) Tiberg, F.; Lindman, B.; Landgren, M. Interfacial Behavior of Nonionic Surfactants at the Silica Water Interface Revealed by Ellipsometry. *Thin Solid Films* **1993**, *234*, 478−481.
(21) Nevskaia, D. M.; Cervantes, M. L. R.; Ruiz, A. G.; Gonzalez, J. D. L. Interaction of Triton X-100 on Silica - a Relationship between Surface Characteristics and Adsorption-Isotherms. *J. Chem. Technol. Biotechnol.* **1995**, *63*, 249−256.
(22) Despert, G.; Oberdisse, J. Formation of Micelle-Decorated Colloidal Silica by Adsorption of Nonionic Surfactant. *Langmuir* **2003**, *19*, 7604−7610.
(23) Li, N. N.; Thomas, R. K.; Rennie, A. R. Adsorption of Non-Ionic Surfactants to the Sapphire/Solution Interface - Effects of Temperature and pH. *J. Colloid Interface Sci.* **2012**, *369*, 287−293.
(24) Drzymala, J.; Mielczarski, E.; Mielczarski, J. A. Adsorption and Flotation of Hydrophilic and Hydrophobic Materials in the Presence of Hydrocarbon Polyethylene Glycol Ethers. *Colloids Surf., A* **2007**, *308*, 111−117.
(25) Schick, M. J. Effect of Electrolyte and Urea on Micelle Formation. *J. Phys. Chem.* **1964**, *68*, 3585−3592.
(26) Han, S. K.; Lee, S. M.; Kim, M.; Schott, H. Effect of Protein Denaturants on Cloud Point and Krafft Point of Nonionic Surfactants. *J. Colloid Interface Sci.* **1989**, *132*, 444−450.
(27) Sagle, L. B.; Zhang, Y. J.; Litosh, V. A.; Chen, X.; Cho, Y.; Cremer, P. S. Investigating the Hydrogen-Bonding Model of Urea Denaturation. *J. Am. Chem. Soc.* **2009**, *131*, 9304−9310.
(28) Li, W. F.; Zhou, R. H.; Mu, Y. G. Salting Effects on Protein Components in Aqueous NaCl and Urea Solutions: Toward Understanding of Urea-Induced Protein Denaturation. *J. Phys. Chem. B* **2012**, *116*, 1446−1451.
(29) Kamei, D. T.; Wang, D. I. C.; Blankschtein, D. Fundamental Investigation of Protein Partitioning in Two-Phase Aqueous Mixed (Nonionic/Ionic) Micellar Systems. *Langmuir* **2002**, *18*, 3047−3057.